Available online at www.sciencedirect.com
ScienceDirect
Physics of the Earth and Planetary Interiors 166 (2008) 203–218
PHYSICS OF THE EARTH AND PLANETARY INTERIORS
www.elsevier.com/locate/pepi

Temporal structure of the global sequence of volcanic eruptions: Order clustering and intermittent discharge rate

A.A. Gusev [a,b,*]

[a] *Institute of Volcanology and Seismology, Russian Ac. Sci. 9 Piip Blvd., 683006 Petropavlovsk-Kamchatsky, Russia*
[b] *Kamchatka Branch, Geophysical Service, Russian Ac. Sci 9 Piip Blvd., 683006 Petropavlovsk-Kamchatsky, Russia*

Received 22 July 2007; received in revised form 10 December 2007; accepted 16 January 2008

Abstract

To study the temporal organization of global volcanic activity over time scales from years to centuries, the following three event sequences were studied: two subsets of the regular catalog of eruptions after Siebert and Simkin [Siebert, L., Simkin, T., 2002. Volcanoes of the World... http://www.volcano.si.edu/gvp/world/], and the "ice core volcanic index" (IVI) sequence, based on the volcanic eruption record as acid layers in big glaciers (Robock, A., Free, M.P., 1996. The volcanic record in ice cores for the past 2000 years. In: Jones, P.D., Bradley, R.S., Jouzel, J. (Eds.), Climatic Variations and Forcing Mechanisms of the Last 2000 Years. Springer-Verlag, New York, pp. 533–546). To perform the statistical analysis in a meaningful way, data subsets were extracted from the original data, with size thresholds and time intervals carefully selected to make these subsets nearly homogeneous. The analysis has revealed, generally, the tendency to clustering, manifested in the following three forms: (1) The event rate is not uniform in time: event dates form active episodes ("common" clusters). (2) In the time-ordered, sequential list of sizes of eruptions, larger events do not appear purely randomly; instead, they form tight groups ("order clusters"). (3) The volcanic products discharge rate is significantly non-uniform, and shows episodic (intermittent or bursty) behavior. It was also found that for the volcanic sequences analyzed, the two types of clustering behavior mentioned in (1) and (2) are positively correlated: larger events are concentrated at the periods of higher event rate. Such a relationship is best demonstrated by the fact that there is clear negative correlation between the following two time series: (1) of the exponent b of the power law size–frequency distribution (the analog of b-value of the Gutenberg–Richter law for earthquakes) and (2) of the current event rate. Power spectra of the analyzed sequences mostly follow power laws, with negative exponent β. Thus, these sequences can be qualified as pulse flicker noises. In other words, they are fractal sequences with correlation dimension $D_c = \beta + 1 < 1$, and both their clustering and episodicity are of self-similar character. The revealed peculiarities of the global volcanic sequence suggest that some global-scale mechanism exists that is responsible for their origin. They are also or primary importance for understanding the impact of volcanism on climate.

Keywords: Volcanic eruption; Sequence; Global; Episodic; Fractal; Clustering; Size–frequency law

1. Introduction

The temporal structure of volcanic processes is interesting in itself, important at least for phenomenological description of observations. If established, the peculiarities of the temporal structure may elucidate mechanisms that are hidden under the observed variety of volcanic phenomena. Also, the probable impact of volcanism on climate can be significantly modified when volcanic aerosol formation is systematically organized in time. One more field where the understanding of the temporal structure may be useful is the study of volcanic hazard. In a number of studies it has been noted that that the temporal structure of volcanism is non-uniform, episodic in time for such processes as ocean ridge volcanism, hot spot volcanism, explosive volcanism in island arcs and trap volcanism (Kennett et al., 1977; Rea and Scheidegger, 1979; Makarenko, 1982; Cambray and Cadet, 1996; Sigurdsson, 2000; Prueher and Rea, 2001). However, these studies analyzed episodicity only in qualitative terms; no formal description for the episodic temporal structure of these volcanic processes was proposed. The described studies did not show specific time scales for episode durations. This may suggest that active episodes arise in time in a statistically self-similar manner. For historic timescales, statistically self-similar or fractal behavior of volcanic eruption sequences has been revealed by

* Tel.: +7 415 22 59510; fax: +7 415 22 59130.
E-mail address: gusev@emsd.iks.ru.

0031-9201/$ – see front matter © 2008 Elsevier B.V. All rights reserved.
doi:10.1016/j.pepi.2008.01.004

Dubois and Cheminee (1988, 1991), and Telesca et al. (2002). A detailed study of fractal space–time structure of intrusions was made by Pelletier (1999).

There are, however, other viewpoints and approaches in the analysis of volcanic eruption sequences. Some studies (e.g., Wickman, 1966; Ho et al., 1991; De la Cruz-Reina, 1991; Jones et al., 1999) either assume or prove that eruptions of a particular volcanic center or of an area behave purely randomly, as a Poisson process. There are also models of non-homogeneous Poisson processes, with variable (deterministic or random) event flux density (e.g., Ho, 1991; Connor and Hill, 1995; Jaquet and Carniel, 2001). Bebbington and Lai (1996) found that the Poission model is valid for one of the two volcanoes studied, but was rejected for another one that showed short-term eruption clustering (or, equivalently, correlation between events); neither of the two manifested long-term memory (and thus fractal behavior). Similarly, Godano and Civetta (1996) found that correlation of Vesuvius eruptions, although observable at short delays, practically disappears at long delays; and Jaquet and Carniel (2001), analyzing seismic activity at Stromboli, found that only short-term memory/correlation is present. Also, tendencies to periodicity of eruptions have been revealed, e.g., by Wickman (1966) who noted cyclic behavior of individual volcanoes, by Ammann and Naveau (2003) who found an expressed 76-year cycle in volcanic activity in tropical zone since 1400 using ice core data, and by Mason et al. (2004) who found a yearly cycle of eruptive activity.

Generally, the multi-scaled clustered behavior is common but not universal tendency, and its presence for any particular data set needs separate analysis. In such an analysis, the problem of data completeness is specifically important. Although some approaches has been proposed for treatment of incomplete data (Guttorp and Thompson, 1991), really convincing results can only be obtained if one is provided with a homogeneous, consistent initial data set.

A few kinds of temporal structure of volcanic event sequences have been mentioned above. To discuss them, more accurate terminology is needed. Consider first the approach when the event size information is ignored. For such cases, we shall further call the tendency of event rate/density to form episodic maxima "common clustering". This term is needed in order to distinguish this kind of behavior from another mode of clustering that we call "order clustering". To observe this second kind of clustering, event sizes should be analyzed along with event times. Observing a sequence of events of various sizes, one can note a tendency of *large* eruptions to appear in clusters (Gusev et al., 2003). These clusters are seen in the time-ordered event list, *with accurate event times ignored*. It is important to realize that this "order clustering" phenomenon is completely independent of common clustering, when *sizes of events are ignored*, and should not be confused with the latter. Order clustering was first revealed in global and regional earthquake catalogs (Ogata and Abe, 1991; see also Gusev, 2005).

Both common and order clustering may be limited to short time/number delays (short-term clustering, with a certain limited correlation time), or to be manifested simultaneously for many time scales, including the longest among those observed. In this latter case we speak of long-term clustering, or long-term memory. In the simplest case, clustering behavior can be organized in a similar way on all analyzed time scales; then we speak of self-similar or fractal behavior (Mandelbrot, 1982). Sometimes, the analyzed range of scales can be divided into sub-ranges with different fractal behavior in each (Dubois and Cheminee, 1993); but data sets studied here are limited in volume and do not permit such a fine analysis.

Generally speaking, clusters of each of the two described kinds may arise independently. Alternatively, they can occur in some organized fashion, e.g., positively or negatively correlated. The actual mode of behavior is unknown, and its study might shed some light on the mechanisms that control the evolution of volcanism. It is difficult, however, to develop this line of study with data sets of the actual size (100–300 events). Therefore, an indirect approach was developed, based on the following observation. During the time segment occupied by an "order cluster", the fraction of large events (among all events) can be expected to be unusually high. This fact suggests that order clusters can affect the size distribution of events. For many kinds of natural (and social) phenomena, the event size distribution is near to power law (Pareto law), and this kind of distribution was also noted for eruption sizes (Turcotte, 1992; Simkin, 1993) as well as for earthquake energies/seismic moments. With respect to earthquake sequences, it is common to monitor size distribution variations through the study of the exponent of the mentioned power law, commonly denoted "the *b*-value". One can expect that this approach can be applied to volcanic sequences as well. This is done in the following, with an unexpectedly definite result: common clusters and order clusters show clear positive correlation.

Speaking abstractly, there is a multitude of modes of possible non-uniform behavior of a volcanic sequence. One of the simplest and often observed forms of such a multi-scaled behavior is the scale-invariant or self-similar behavior. Such processes are called fractal time sequences, or flicker noises (see e.g. Mandelbrot, 1999). The fractal behavior of natural and artificial phenomena attracted very wide attention recently in many fields of science; a number of studies were listed above that suggest that the formation of fractally organized clusters may be considered to be a reasonable initial hypothesis in the study a volcanic sequence. For this reason, in the following analysis the fractally clustered or intermittent behavior is considered as a main alternative to the uniform, non-clustered behavior. Recently, updated versions of two important data sets representing global volcanic activity has been kindly made available for me by their authors. In the following, these global data sets are used to achieve better understanding of the temporal behavior of global volcanism over time scales from months to hundreds of years.

When event dates and sizes are combined in a catalog of events, they define the temporal structure of the output of eruption products, further called volcanic discharge. Through the accumulation of volcanic material and thus formation of volcanic rock sequences, this output determines, to a large degree, the geological effect of volcanism. Its analysis is critical for

possible comparison to geological history because individual eruptions rarely can be identified in the geological record.

Generally speaking, the rate of accumulation of eruption products may be uniform or demonstrate some specific behavior, e.g., to be periodic or, oppositely, an episodic/clustered one. The above-mentioned studies based on volcanic rock successions often demonstrate the episodic behavior of volcanism in time. It is interesting to find out whether this behavior can be seen in the dated volcanic event sequences. Therefore, possible fractal structure of volcanic discharge shall be analyzed in parallel with the study of clustering.

The organization of the paper is as follows. It begins with general discussion of temporal properties that can be expected for eruption sequences. Initial data and their preprocessing are then described, and three data subsets are specified. Further, for all these subsets, event rate variations, order clustering, volcanic product discharge rate and b-value variations are analyzed. The reality of all these modes of behavior shall be shown for all or at least for two of the three analyzed sequences. Each of these analyses is prefaced by discussion of the particular processing procedure. Lastly, joint analysis of results is given, over various analyzed features and over data sets.

2. Known and possible peculiarities of temporal structure of volcanic event sequences

Before considering possible features of temporal behavior of volcanic event sequences, data selection criteria must be discussed. One can note that data selection standards have not yet been settled in this field. The studies of seismicity can make a model in this respect. In seismology, both historical and recent (instrumentally studied) events are quantified by magnitude value. To guarantee that data subsets are uniform, the total catalog duration is divided into subperiods of approximately constant degree of completeness. A certain magnitude threshold is selected for each subperiod so that events above this threshold can be considered as nearly complete. Such an approach makes seismicity data acceptable for statistical analysis. In the case of volcanic eruption data, their homogeneity can be violated by gaps in reporting, inaccurate event size quantification, time-variable data selection criterion, etc. If, by measures exemplified above, a volcanological data set under analysis is not made homogeneous, one can easily encounter temporal peculiarities that are no more than artifacts emulating properties of natural origin. An additional requirement, specific for volcanology, is that the history of volcanic activity should be representable as a sequence of dated individual events of negligible duration; this shall be assumed for the data sets under study.

To fulfill the listed requirements, first a certain size parameter must be ascribed to each eruption event. We assume that this very important step has already been performed by data compilers. Second, a certain lower threshold must be set for event size, to provide data completeness. Both these requirements can be fulfilled only approximately with real data, because the accuracy of size estimates of eruptions is limited, and because the smaller is an event, the larger are chances for it to be unreported. Although selecting a high threshold for size might minimize the probability of gaps in data, it also minimizes data volume, often making statistical analysis impossible. Thus, some compromise is needed when selecting the threshold. One important practical requirement is that the threshold must be stable for entire time span of the analysis. With indefinite, uncertain and/or time-dependent threshold for data selection, any quantitative data analysis may become (and sometimes do become) mostly meaningless.

To verify at least approximate homogeneity of a data set, one can use the following two tests. The first one, that follows the practice of seismicity studies (cf. also Gusev et al., 2003), is based on the assumption that the size distribution (size–frequency law) for eruptions follows the power law (Turcotte, 1992; Simkin, 1993) This law can be written either in a differential form (for histogram $n(\cdot)$), or in an integral form (for cumulative sum $N(\cdot)$):

$$n(10^{-0.5}V < V' < 10^{0.5}V) = a_{\mathrm{d}} - b\log_{10}(V) \tag{1a}$$

$$N(V' > V) = a_{\mathrm{c}} - b\log_{10}(V) \tag{1b}$$

where V is a certain measure of the amount of eruption products that quantifies the eruption size. In the following this measure will be called "volume"; generally, other measures, like mass or energy may be more adequate, but this point is outside the scope of this paper. The observed value of the exponent b in (1a) and (1b) is mostly in the range 0.6–1. Of course, this law is not strict; but when for a certain data set it is clearly violated (e.g., $n(V)$ does not decrease monotonically), this strongly suggests incompleteness of this data set.

Another way to verify the completeness of data is to check whether the event rate is approximately uniform. In the quite common case when the event rate systematically increases as time approaches to the present moment, one can strongly suspect a drifting (decreasing) lower threshold of event size or, more or less equivalently, a gradual increase in the degree of completeness of smaller-size events. It must be noted that both proposed data checks are informal: natural data may deviate from the ideal size–frequency law (1); also the constancy of the small-event rate can be no more than approximate (its natural variations form just the above-discussed clusters). Only when a data set can pass the mentioned checks, one can try to analyze its temporal structure. With real data, this practically means that an approximately uniform subset of data must be selected for analysis, with a certain time window and with a certain lower bound on event size.

The best-known sort of temporal structure is a non-uniform event rate, manifested, e.g., as a systematic drift of the average event rate. In other cases, there is no evident trend, whereas the deviations from purely random timing of events are present. These deviations may have various forms as, e.g., a tendency to periodicity, or a tendency to the clustered or burst-like behavior, or expressed as stochastically varying event density. The tendency of event dates to form tight groups/clusters on the time axis, or, equivalently, for event rate to form clear maxima, is called "common clustering" in the following.

Another, less-known tendency may appear in a sequential list of event sizes, when one takes into account only the order of

occurrence and ignores accurate dates. In this list, events of different sizes can be distributed completely randomly, or show some structure. (A fully artificial example is the occurrence of events in the order of their sizes: the smallest, the second smallest, etc.) A kind of structure that was found to be actually present in volcanic (and earthquake) sequences is "order clustering", or the inherent tendency of the largest events to occur "too often" as close neighbors in the time-ordered list. ("Too often" means "significantly more often than expected for a randomly shuffled event list".) Accurate timing is irrelevant for order clustering, in contrast to "common" clustering when the rate of events, whose size is now inessential, varies in time, producing in particular event rate maxima, or equivalently tight groups or clusters. See Gusev et al. (2003) for an example of order clustering of eruptions and for the detailed discussion of this phenomenon.

The order clustering behavior has much in common with temporal variation of *b*-value. Indeed, a time segment with unusually high number of large events must have unusually flat graph of size–frequency distribution, that is, unusually low *b*-value. The close connection between order clustering and *b*-value variation provides a convenient way to study the temporal relationships between common and order clustering (avoiding the awkward problem of identification of individual clusters). When both common and order clustering are present in data, one can ask whether their time variations match (are in phase), or "anti-phased", or show no simple correlation. To perform such an analysis, one usually coverts a data set into a sequence of intervals; then he must apply a tool that can ascribe to each window its degree of common and order clustering. The natural measure of common clustering is the local estimate of event rate. And to measure the degree of order clustering one can use just the local estimate of *b*-value.

A significant aspect of the time structure of volcanic sequences is the character of the discharge of volcanic products. Like event rate, volcanic discharge rate (VDR) can be uniform, monotonously or randomly drifting, etc. Speaking of episodic or intermittent behavior of VDR, one should clearly distinguish three factors that control its irregularity: (1) short eruption events as opposed to inactive background (may become disputable for long-duration eruptions); (2) heavy-tailed size distribution of eruption sizes (Eqs. (1a) and (1b)), resulting in the dominant contribution of the largest events into the long-term-averaged VDR; and at last (3) episodic temporal behavior proper. It is the latter factor that is under study in this paper.

The listed features of the temporal structure of volcanic sequences are not independent. For example, both the episodicity of event rate and order clustering, each operating separately, would result in the episodicity of VDR. If both factors are present, the outcome is less definite. When order clusters match maxima of the event rate, the two phenomena shall amplify one another, resulting in the enhanced expression of episodicity of VDR. Oppositely, when order clusters match minima of event rate (the case of anti-correlation of the two types of clustering), episodicity of VDR shall be reduced or even completely suppressed. Thus, all parameters of the temporal structure must be analyzed jointly.

3. Initial data sets and extraction of nearly homogeneous subsets from them

3.1. Initial data sets

The first data set analyzed is the well-known global catalog of volcanic eruptions of the Smithsonian Institution (Siebert and Simkin, 2002; see also Simkin and Siebert, 1994). Lee Siebert kindly provided its recent version (as of 2004), labeled SMI in the following.

Another data set to be considered here is the record of volcanic activity of the last centuries as fixed in of the ice core volcanic index (IVI) proposed and compiled by Robock and Free (1996; see also Robock, 2000). Alan Robock (personal communication, 2004) kindly provided the most recent version of this data set. Determination of IVI uses dated annual layers of the ice extracted from boreholes in big glaciers. Some of these layers contain H_2SO_4 of presumably volcanic origin. The IVI list was produced by critical compilation of acid layer sequences found in a number of locations in Northern and Southern hemispheres. The acid layers are formed by the following mechanism: an explosive eruption forms an eruption column that penetrates the stratosphere and there injects SO_2 that is oxidized to SO_3 forming finally H_2SO_4 droplets; this aerosol is dispersed, by stratospheric winds, not quite uniformly, over the respective hemisphere and, in smaller amounts, over the opposite hemisphere; aerosol slowly settles making local precipitation (snow) marked by greatly increased H_2SO_4 content; the snow accumulates and is buried to form a layer in a glacier. The characteristic times are weeks to months for aerosol dispersion and about 1 year for aerosol settling. Many factors prevent the local H_2SO_4 content to be a completely reliable indicator of volcanic activity. The main two of these factors are an unstable relationship between the size of eruption and the amount of H_2SO_4 injected into the stratosphere and the non-uniformity of global-wide aerosol dispersion and accumulation. The last factor has been partly overcome by matching records from geographically distant glaciers.

As for the physical meaning of IVI, it is the estimate of average optical extinction length of the atmosphere (measuring light absorption related to suspended volcanic aerosol). For ideal conditions, IVI values must be proportional to the amount of optically active aerosol. An important feature of the IVI data is that they are completely independent of the SMI data. Despite a certainly limited accuracy in representing global explosive volcanism, IVI is its important and valuable indicator; thus it is chosen as one of the objects of the present study.

It must be noted that neither VEI nor IVI are the perfect measures of eruption size. In particular, IVI in principle cannot not reflect even large lava eruptions: they produce no or low stratospheric aerosol. Also, definition of "explosivity" included in the determination of VEI may be an imperfect indication of the total amount of products of a particular eruption. Even in the better-documented cases, the choice still is not finally resolved between size definitions based on mass or volume of products. Still, the data sets we use are the best available.

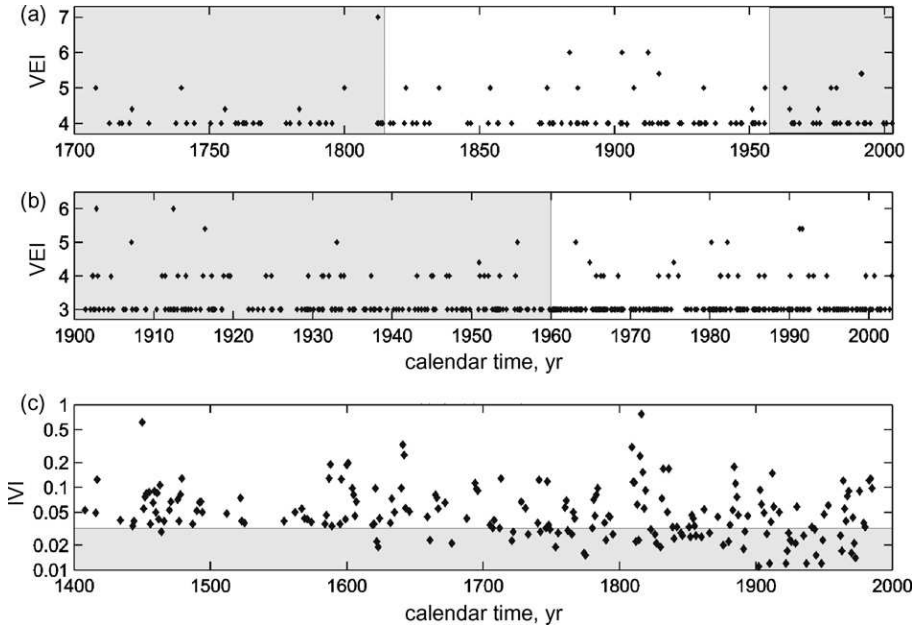

Fig. 1. Original data and selection of approximately complete data segments. (a) Data source SMI, data shown from 1700 with VEI ≥ 4, the selected period is 1820–1960, a data gap can be suspected during Napoleonic wars; (b) data source SMI, data shown from 1900 with VEI ≥ 3, the selected period is 1960–2003; (c) data source IVI, data are selected with IVI ≥ 0.33 for the entire time period.

3.2. Preparing quasi-uniform subsets of the SMI data set

The SMI data set includes the eruption date (of variable accuracy) and the eruption size parameter VEI ("volcanic explosivity index"). VEI reflects the amount of erupted products. VEI is an approximately logarithmic measure of the size if eruption. To form numeric representation of size, we use size parameter $V = 10^{VEI}$. To represent numerically the cases when VEI data were given as "4+" or "5+", the size parameter was doubled. Events with no month indicated were ascribed to July 1. On Fig. 1a and b one can see the present level of completeness of global volcanic data. Visual inspection suggests selecting the following approximately complete data subsets: VEI ≥ 3 since 1960 (event number $N = 226$, further denoted SMI3), and VEI ≥ 4 since 1820. In order to have independent data sets, the data set of VEI ≥ 4 events was limited by time span 1820–1960; it consists of $N = 72$ events and further denoted SMI4. Size–frequency distributions for the periods 1960–2002 and 1850–1960 (Fig. 2) are sufficiently near to power laws and support these selections.

3.3. Preprocessing IVI data set

The original version of the IVI data set consisted of two lists of yearly IVI values for 1400–1986 for each hemisphere, further denoted as IVI_{NH} and IVI_{SH}. To obtain the global data set, these two lists were merged. For years with non-zero records for both hemispheres (related either to a single eruption affecting both hemispheres, or to synchronized eruptions in each of them), one must combine the two values in some way. Two evident ways to do this are to take the maximum of the two values, or to add them. The first way seems to produce underestimates; and another may produce overestimates. As a trade-off solution, the following global index (having no physical meaning, but serving the limited aim of reasonable combination of two single-hemisphere data sets) is further used:

$$IVI_{GL} = (IVI_{NH}{}^2 + IVI_{SH}{}^2)^{0.5} \quad (2)$$

Fig. 1c represents IVI_{GL} values in time. The lack of temporal uniformity of data can be easily seen as the paucity of points in the lower-left part of the plot. Fig. 2 gives the size–frequency distribution in the forms of a histogram and of a cumulative plot. One can see that Eqs. (1a) and (1b) are approximately valid within the IVI_{GL} range from the largest values down to $IVI_{GL} = 0.03$–0.04, and then a clear tendency to saturation is seen, indicating that the original IVI record tends to become incomplete here. In the following, the subset of the IVI_{GL} sequence with $IVI_{GL} \geq 0.033$ is analyzed, further denoted merely IVI. It contains $N = 146$ non-zero yearly IVI records. As an event size measure V, the value of IVI was used directly. In reality, more than one eruption could contribute to a single IVI value; this kind of distortion was inevitable with these data.

Many of the yearly IVI records form continuous chains extending for two or more years. Some of them must be related to the slow settling of aerosol, while others, and especially those with the length of 3 years and more, seem to reflect real sequences of eruptions in successive years. To be on the safe side, in the data analysis a technique will be applied that permits one to accurately cut off the contribution to clustering over short time intervals. A particular value of the shortest delay that is permitted to have effect on our results is selected as 3 years.

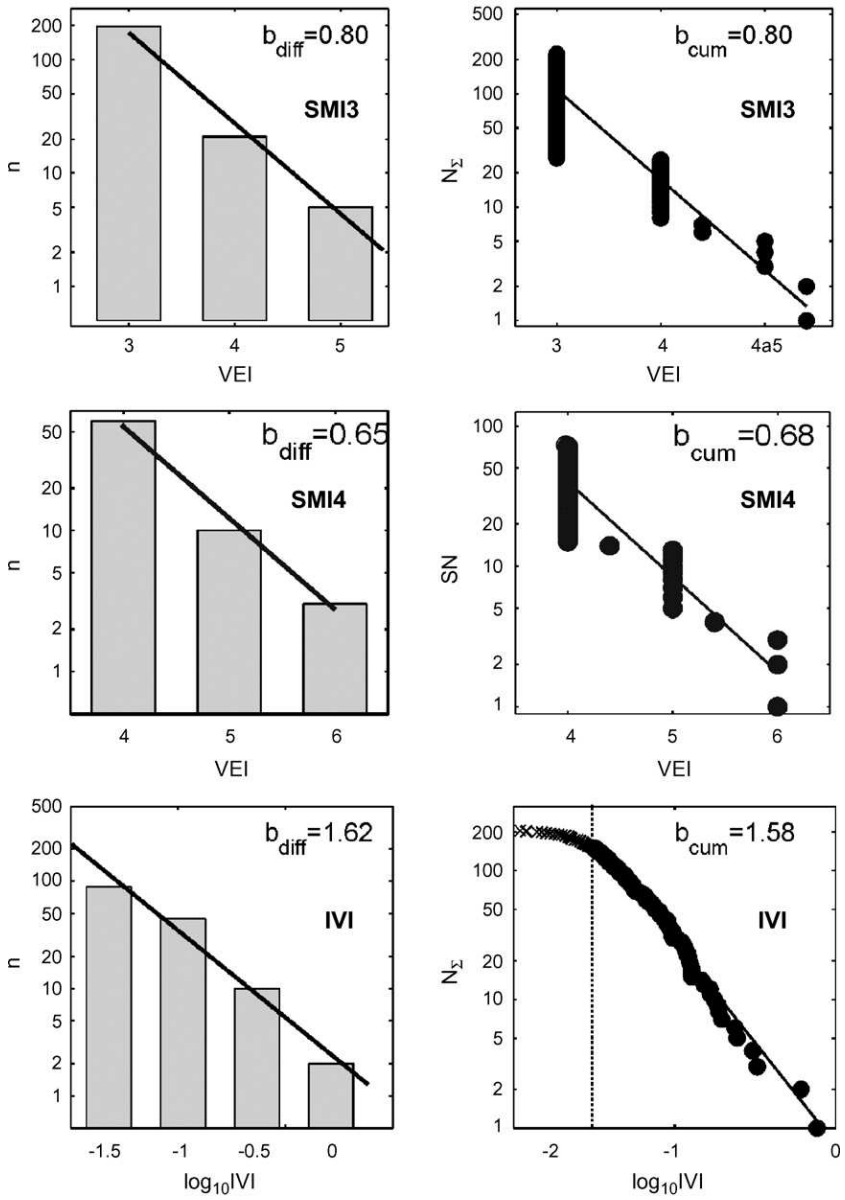

Fig. 2. Size–frequency relationship for data sets IVI, SMI3 and SMI4. (Left column) Histogram-like plots, with bar height proportional to log event number in a bin, see Eq. (1b). (Right column) Cumulative plots, proportional to log cumulative event number (related to complementary cumulative distribution function), see Eq. (1a). Lines are linear fits; their slopes are the estimates of *b*-values given on the graphs. The vertical dash line shows the cutoff value of IVI, equal to 0.033. Only the IVI values above the cutoff were included into the histogram and into the calculation of *b*-value. Note an acceptable fit of distributions by the law (1).

4. Event rate variation and common clustering

4.1. Procedures of analysis

There are many ways to reveal multi-scaled event rate variations, e.g., variogram analysis (Jaquet and Carniel, 2001) or multifractal analysis (Godano and Civetta, 1996), but we needed one that would permit us to go around the problem of short time intervals, that complicates the analysis of IVI data set. The presence of correlation at small time intervals is a result of finite aerosol settling time; this signal must be screened. For this reason, spectral analysis of a data sequence was applied, so that probably biased spectral components could be simply filtered out. The sequence of event dates was represented as a function of time consisting of identical spikes (delta-like pulses) of *unit* amplitude. This data representation is denoted symbolically as $1(t)$. In the case of uniform event rate (purely random or Poisson process), mean power spectrum $P(f)$ of a $1(t)$ function is constant ("white"). In the case of periodicity, spectral spikes appear. In the case of self-similar bursts of event rate, $P(f)$ is power law or hyperbolic one ($P(f) \propto f^{-\alpha}$, with α values typically between 0 and 1.5. This case is known as "pulse flicker noise" with "pink" power spectrum ("pink" because of enhanced low frequencies). In a multifractal context, $1-\alpha$ is equal to the correlation dimension $D_c = D_2$. To detect a pink spectrum in real data, one must test the hypothesis "$\alpha > 0$" against the null hypothesis "$\alpha = 0$", that corresponds to flat ("white") $P(f)$, $D_c = 1$ and the lack of fractal clustering. A usual approach is to

select a set of particular frequencies f_i; and to find, for each f_i, the estimate $P_e(f_i)$ of spectral density $P(f)$ in the neighborhood of f_i by averaging the observed power spectrum $P_o(f)$ (periodogram of data) over a frequency window centered at f_i. Then, specifically for the assumed power law spectral shape, linear regression of $\log P_e(f_i)$ versus $\log f_i$ is then performed, and the slope of the regression line provides the estimate of $-\alpha$. This approach, however, performs badly at lowermost frequencies where important information regarding scaling of the spectrum is located. An alternative approach (Pisarenko and Pisarenko, 1991) is to integrate $P_o(f_i)$ numerically, obtaining the integrated power spectrum $IP_o(f_i)$. In the case of power law spectrum, IP(f) behaves as $f^{-\alpha+1} = f^{-\alpha'}$. When analyzing scaling behavior of the spectrum, it is useful to equalize the relative contributions to the result of different frequency bands that cover the logarithmic frequency axis. A typical example of this approach is to use octave bands. We need denser grid, and actually use three points per octave, or ten points per decade. Ideally, we would like to estimate the integrated spectrum $IP_o(f)$ at points f_j that form a geometric progression $f_{j+1} = af_j$, with the ratio $a = 1.259 = 10^{0.1}$. This aim cannot be realized literally however because our raw spectral estimates $P_o(f_i)$ are located at certain frequency points f_i that are separated by a fixed frequency step $1/T$, and form *arithmetical* progression. Thus, out of the set of points f_i we must select a subset f_j that is near to geometric progression. Then, linear regression is performed with pairs $\{\log f_j, \log IP(f_j)\}$. The actual set of frequency points used can be written as $f_j = (1/T)\{1, 2, 3, 4, 6, 8, 10, 12, 16, 20, 25, 32\ldots\}$. Regression delivers the estimate of $\alpha' = \alpha - 1$ and therefore of α. It should be noted that in empirical discrete IP(f_j) functions, the accuracy of the first one to two points is inevitably very low; thus even marked deviations of these points from the straight regression line are tolerable, and cast no doubt on the validity of linear regression.

The estimate of α must be accompanied by error bounds (or, better, by distribution density) that would permit one to formally test the hypothesis "$\alpha > 0$". To produce these error bounds analytically is not straightforward even in the asymptotic case of a very large data set; in the case of a real small data set it is a difficult task. To overcome this problem (relevant not only for the α parameter), Monte-Carlo estimates of distributions of analyzed parameters for the case of null hypothesis are systematically used in the following. To obtain these, the actual temporal structure of events is substituted by many copies of a randomized one. Sets of artificial event dates ("surrogate data") are generated as realizations of Poissonian sequence, and each surrogate data set is processed using the same procedure as one applied to real data. Empirical distribution function of α estimates determined on the basis of 1000–10,000 realizations of a data sequence with true $\alpha = 0$ approximates the α distribution for the case of the null hypothesis. To determine the significance level of the hypothesis $\alpha > 0$, the value α_{ob} obtained from observed data is used as a boundary value, and the empirical distribution function is integrated from α_{ob} to infinity, resulting in the estimate of probability of realization of the event $\alpha > \alpha_{ob}$ on the condition that the null hypothesis is true; by definition this is the significance level Q for the hypothesis in question ("$\alpha > 0$"). Traditionally, round critical significance values for Q are selected like 1%, 2.5%, etc; in our case a value of Q is the output of our procedure and does not take any preferred values. Additional use of Monte-Carlo simulation is the determination of bias in numerical estimation of α caused by small sample sizes (it could reach 0.07–0.09 for the case SMI4 with only 74 events), the resulting estimates of α were adjusted to compensate for this bias. See Gusev (2005) for more detail.

Generally, spectral analysis of data is a standard tool to reveal periodicity. A clear 76-year cycle was detected by Ammann and Naveau (2003) after special preprocessing was applied to the same data sets (IVI_{NH} and IVI_{SH}) as studied here. The present analysis did not reveal any marked periodicity.

After this introduction let us consider individual data sets.

4.2. SMI3 data set

On the size-time graph of this data (Fig. 3a), one can see, in particular, the sequence of event dates. These dates look to be distributed somewhat non-uniformly, but it is not clear how improbable is to obtain a sequence of similar appearance by purely random dispersion of points along the time axis. For spectral analysis applied to possible common clustering, a discrete fine time scale was used with a small arbitrary time step of $T/2048$, and discrete Fourier transform (DFT) was performed on 2048 points. On Fig. 4a one sees the integrated spectrum IP(f) that can be approximated by a straight line with the slope 0.92. In corresponds to slightly pink noise, indicating some tendency to clustering of event dates. The estimate of α equals to 0.08. The significance check was performed for the frequency range 0.25–10 year^{-1} (period range 40–0.1 years, the shortest period selected according to the typical time accuracy of SMI3).

The formal significance level Q for the hypothesis "$\alpha > 0$" was derived from the Monte-Carlo simulation explained above. (See Table 1 for significance values related to all kinds of spectral analysis.) Among 5000 surrogate data sets, as many as 686 produced $\alpha > 0.071$; thus the average significance level is approximately $Q = 686/5000 \approx 14\%$. Thus, although the event rate shows some clustering tendency, its significance is marginal.

4.3. SMI4 data set

On the time–size graph Fig. 3c, one can notice groups of points, but formal analysis based on Fig. 4d, indicates that the clustering tendency is actually not definite. The basis for selection of the upper frequency equal to 0.1 year^{-1} (period 10 years) is discussed below. For the hypothesis "$\alpha > 0$" $Q = 27\%$ is obtained, so the hypothesis cannot be accepted reliably. Qualitatively, estimated $\alpha = 0.16$ agrees with the idea of clustering.

4.4. IVI data set

On the time–size graph (Fig. 3e) one notices rather clear non-uniformity of event dates. On Fig. 4g the regression line is seen for the integrated spectrum, plotted and analyzed only for frequencies below 0.333 year^{-1}. In this manner, all possible contributions of inter-event delays shorter than 3 years are cut off, so that even a 2-year aerosol staying in the stratosphere can-

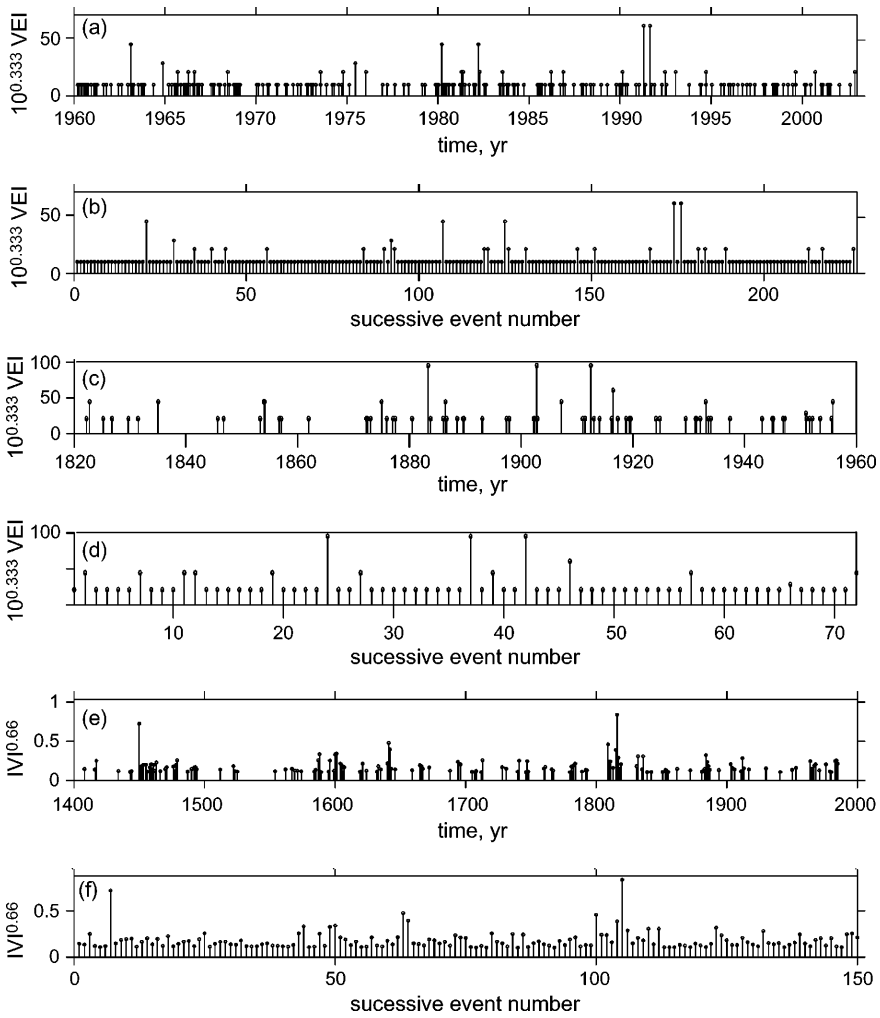

Fig. 3. Distrubutions of event sizes in time (a, c and e) and as a function of sequential event number (b, d and f), for data sets: SMI3 (a and b), SMI4 (c and d) and IVI (e and f).

not imitate the analyzed episodicity. One can see that integrated spectrum corresponds to slightly pink noise, with the estimate of α equal to 0.13. Monte-Carlo estimate for the formal significance level Q for the hypothesis "$\alpha > 0$" equals 10% again indicating a noticeable tendency to "common" clustering.

5. Order clustering

5.1. Procedure of analysis

As was explained above, "order clustering" is the clustering tendency as observed in the time-ordered list of event sizes. This list is treated as a discrete function of sequential event number, this function is denoted symbolically as $V(i)$. Again, spectral analysis is applied to this function. To make frequency scales on the spectral plots approximately comparable, the integer "dates", denoted i above, are multiplied by the value of an artificial time step, equal to the average inter-event interval. (This modification is irrelevant for the formal analysis of significance.) The resulting time scale is denoted as t^*. The argument of the Fourier transform of $V(t^*)$ is denoted f^*. Now consider the function $V(i)$ (or $V(t^*)$). When the sequence of sizes is random, $V(t^*)$ is a white (non-Gaussian) noise, whereas when the order clustering is present, $V(t^*)$ is intermittent. Moreover, when clusters have no preferred scale on the t^* axis (what is highly probable), $V(t^*)$ may be a pink noise. To reveal its presence, the approach developed above with respect to the event rate analysis can be applied, with the following minor modifications. The first change, a technical one, is that when analyzing $V(i)$ a DFT on N points is used. The analytical technique described for the case of $P(f)$ is then applied: the $V(f^*)$ spectrum is integrated obtaining $IV(f^*)$; then, the value of α in the relationship $IV(f^*) \propto f^{-\alpha+1}$ is estimated by linear regression of $\log IV(f^*)$ versus $\log f^*$. As a final step, the significance level for the hypothesis "$\alpha > 0$" is checked by a Monte-Carlo approach with surrogate data. In this case, in order to generate surrogate data sets with no temporal structure, it is useless to perturb times of events (they are fixed); instead, the time-ordered list of event sizes is randomly shuffled many times.

5.2. SMI3 data set

To determine the significance of order clustering, the just described procedure is performed, see Fig. 3b for size–number plot and Fig. 4b, for the $\log IV(f^*)$ versus $\log f^*$ graph. The shape

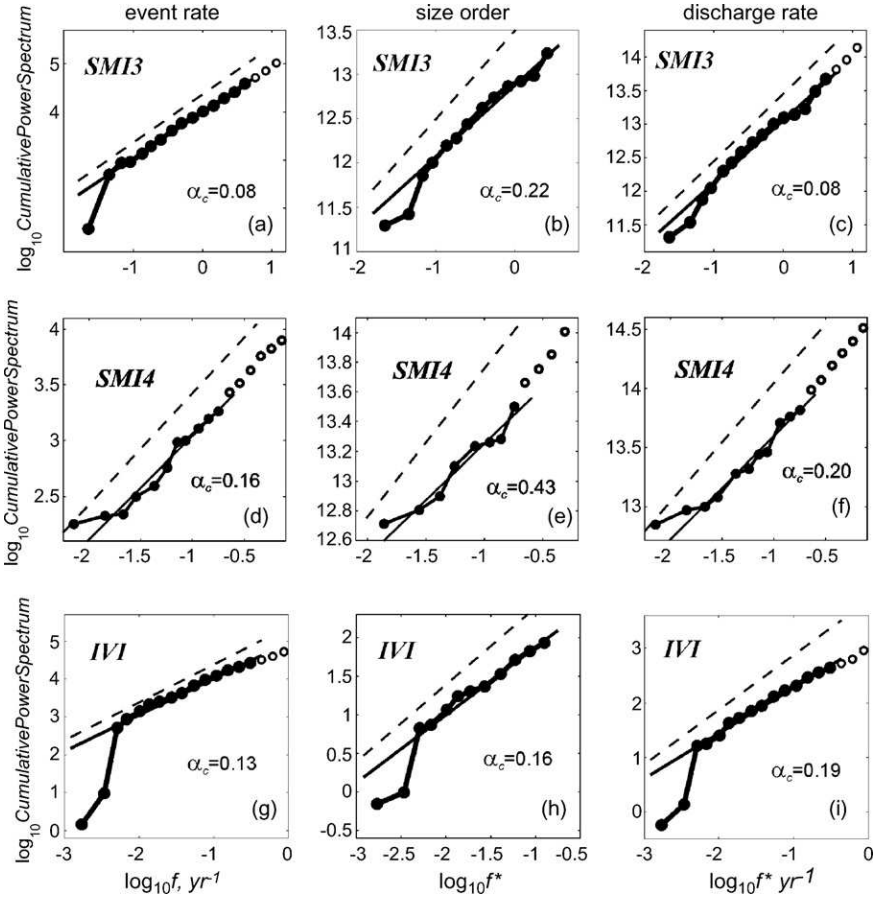

Fig. 4. Integrated power spectra IP(f) calculated from IVI, SMI3 and SMI4 data sets (dots). Left middle and right columns corresponds to "1(t)", "$V(i)$" and "$V(t)$"data sequences, respectively. Middle column corresponds to the time–size plots of Fig. 3(b, d and f). Right column corresponds to the sequences of Fig. 3(a, c and e). Dashed lines, with slope unity, are for the reference case of "white" power spectra ($P(f) = \text{const} \propto f^0$, $\text{IP}(f) \propto f^1$) that have no temporal structure. Solid straight lines are power law fits of calculated spectra. Circles are data points excluded from linear fitting, see text for clarification. Units on vertical scales are arbitrary.

Table 1
Spectral slope parameter α and related parameters, estimated through integration of observed power spectra

Processing mode	α	D_c	$\sigma(\alpha)$	Q (%)	Q_{st} (%)
Data: SMI3, $N = 226$, $V = 10^{\text{VEI}}$, $f_{up} = 10\,\text{year}^{-1}$					
1(t)	0.08	0.92	0.06	14	15
$V(i)$	0.22	0.78	0.09	2.1	2.5
$V(t)$	0.08	0.92	0.05	5.9	10
Data: SMI4, $N = 72$, $V = 10^{\text{VEI}}$, $f_{up} = 0.2\,\text{year}^{-1}$					
1(t)	0.16	0.84	0.23	27	–
$V(i)$	0.43	0.65	0.30	11	15
$V(t)$	0.20	0.80	0.20	16	20
Data: IVI, $N = 146$, $V = \text{IVI}$, $f_{up} = 0.33\,\text{year}^{-1}$					
1(t)	0.13	0.87	0.09	6.7	10
$V(i)$	0.16	0.84	0.12	8.9	10
$V(t)$	0.19	0.81	0.09	1.7	2
Average over data sets					
1(t)	0.09	0.91	0.050		
$V(i)$	0.20	0.80	0.072		
$V(t)$	0.11	0.89	0.044		

α, estimated exponent of the power law in the power spectrum; $D_c = 1 - \alpha$, estimated correlation dimension; $\sigma(\alpha)$, rms deviation of the α estimate; Q, calculated significance level for the hypothesis $\alpha > 0$; Q_{st}, same, rounded up to a traditional standard level; dash: the case of no significance.

of the integrated spectrum is well described by a straight line, and its slope of $0.78 < 1$ indicates a clear tendency to clustering. Deviations of the first two points can safely be ignored, as was mentioned above. For numerical results see Table 1. The obtained significance level is $Q = 2.1\%$, suggesting that the hypothesis of multi-scaled order clustering agrees with the data reasonably well.

It must be noted, however, that to obtain this seemingly convincing significance level, it was important that the 1991 doublet eruptions (Pinatubo and Cerro Leon) are specified as having VEI = 5+, not 5, and ascribed, correspondingly, an increased value of "size" V. If the components of this close group (representing the only two VEI = 5+ eruptions of 1960–2002) were considered as having VEI = 5 (making all five largest eruptions of 1960–2002 equal to one another), the significance level would change to much less impressive 17%, still indicating that this or larger degree of order clustering can appear purely randomly only once in six cases.

5.3. SMI4 data set

The $V(i)$ graph (Fig. 3d) shows one clear but relatively long 1883–1907–1912 cluster (Krakatau, Santa-Maria, Katmai) and no compact clusters. The spectral shape (Fig. 4e) deviates

from unity only below the frequency of 0.2 year^{-1} ("periods" $1/f^*$ above 5 years). At higher "frequencies", the spectrum is white, and the general spectral shape is curved. Therefore, only the presence of clustering can be checked in this case; but the assumption of *self-similar* clustering behavior is not supported by these data. To test the hypothesis of clustering, the analysis was limited only by "frequencies" $f^* < 0.2$ year^{-1}. For this frequency band, $\alpha = 0.43$ with very low accuracy, and $Q = 11\%$; thus, order clustering is expressed, but only moderately.

5.4. IVI data set

On Fig. 3f one sees the $V(i)$ graph that shows evident bursts suggesting the presence of order clustering. The $\log IV(f^*)$ versus $\log f^*$ graph of Fig. 4h is analyzed for "frequencies" below $f^* = 0.33$ year^{-1}; in this way possible bias related to small time intervals is suppressed. Over this band (in fact, in a wider band), the spectral shape is well approximated by a straight line (of slope 0.84), making the assumption of self-similarity of clustering reasonable in this case. Based on the obtained significance level $Q = 9\%$, one can conclude that the hypothesis of self-similar ordered clustering is reasonably supported by the data.

6. Burst-like discharge of volcanic products

6.1. Procedure of analysis

To study VDR, the data sequence was represented as a time function consisting of spikes (delta-like pulses), in the same manner as with common clustering, with the evident change that a spike has now the amplitude equal to event size, instead of unity. The result is denoted as $V(t)$. To destroy temporal structure when generating surrogate data, both mentioned randomizations are now made: actual dates are substituted by a Poisson sequence, and the time-ordered event list is randomly shuffled. All other steps are as before.

6.2. SMI3 data

See Fig. 3a for original data over time axis and Fig. 4c for the spectral shape and regression line of $\log IV(f)$ versus $\log f$ dependence. The observed spectrum is well fit by a straight line, whose slope indicates pink noise with $\alpha = 0.08$. The Q value is 6%, suggesting that self-similar episodic behavior of VDR is probable for SMI3 data.

6.3. SMI4 data

For this data set (Fig. 3c), similarly to the case of the analysis of $V(i)$, the episodic behavior for VDR is suggested by the spectral shape (Fig. 4f) only for sufficiently low frequencies (periods longer than 5 years). The significance level is not convincingly low (only 16%), making the conclusion regarding episodic behavior not fully reliable in this case.

6.4. IVI data

See Fig. 3e for original time structure of data. The observed spectrum Fig. 4i is well fit by a straight line, whose slope indicates pink noise with $\alpha = 0.19$. The Q value is below 2%, thus, the reality of episodic behavior of VDR is well supported by the data in this case.

7. Correlation in time between common and order clusters

7.1. General approach

It was noted above that the relationship between degrees of expression of common clustering (=event rate variations), order clustering and VDR variations suggests that the two first phenomena may act cooperatively to enhance the third one. It was also noted that this idea of "cooperation" can be checked considering the relationship between event rate variations and b-value variations. In particular, event rate maxima, or common clusters, must coincide in this case with groups of larger-sized events, and such groups must cause the local b-value to be *low*. Therefore, the hypothesis of "cooperation" predicts *negative* correlation in time between event rate and b-value.

To implement the described idea, the following technique of data processing is used. The time-ordered list of N events is cut into a sequence of K packets, each containing the same fixed number M of events. (A few events in the end of the list that do not form a complete packet are dropped.) The duration of ith packet equals dt_i, $i = 1, 2, \ldots, K$. For ith packet, the local event rate estimate is evidently $\lambda_i = M/dt_i$, and the local b-value estimate by maximum likelihood (Aki, 1965) is

$$b_i = \log_{10} \mathrm{e} \left[\frac{(\Sigma_i \log V_i)}{M - \log V_0)} \right]^{-1} = \log_{10} \mathrm{e}[\bar{m} - \log V_0)]^{-1} = \tag{3}$$

where V_i denotes the size of ith event, V_0 is the lower threshold used in V_i selection, and $\bar{m}$ is the average logarithm of event size in the data subset, further called "average magnitude". In the analysis of correlation between λ_i and b_i, one meets with the tradeoff between the accuracy of λ_i and b_i that requires large M (and thus small K), and the accuracy of correlation coefficient ρ that requires the opposite. In this situation, the near-optimal choice is to select both K and M of the order of $N^{0.5}$.

With very scarce data available, the results of such an analysis are prone to large statistical fluctuations. To reduce their effect, two modifications are introduced. First, the number of λ_i and b_i estimates is doubled, by using 50%-overlapping of packets. (That is, with e.g., $M = 8$, successive packets include events with $i = (1, 2, \ldots, 8)$,$(5, 6, \ldots, 12,)(9, \ldots, 16)$, $(13, \ldots, 20)$ and so on.) Second, the analysis is repeated with several variants of M value. Additionally, it was found that with small data sets, it is preferable to directly use the $\bar{m}$ statistic and not to convert it to b-value. Negative correlation between λ_i and b_i means positive correlation between λ_i and $\bar{m}_i$. (Intuitively this is transparent: high event density is correlated to high aver-

age log event size.) Then, correlation is analyzed between time series λ_i and $\bar{m}_i$, both visually and through statistical testing. We expected that $\rho > 0$, and tested this hypothesis against the null one "$\rho = 0$". Again, a Monte-Carlo technique with surrogate data sequences (made of uniformly distributed points with shuffled size order) was applied to determine the significance level.

Although this mode of data analysis is straightforward and intuitively attractive, its detection power appeared to be poor with the actual volumes of the data sets. Another, less transparent but more susceptible technique was also applied: b-values were determined for two specially selected subsets of events and then intercompared. The first subset included events that are located in densely populated intervals of time axis; another, oppositely, includes events from sparsely populated intervals. To sort events according to the population type of their interval, an estimate of density is associated with each event. For the ith event, this density is estimated as the inverse of the time interval $t_{i+2}-t_{i-2}$ between the two next nearest events. In this way, all events were sorted into two subsets of equal size, and b-values were determined for each subset. The critical parameter is the difference between b-values of the two subsets. A Monte-Carlo technique was applied again to test the hypothesis that among two b-value estimates, the one that is related to denser intervals has the lower of two b-values.

7.2. SMI3 data set

On Fig. 5a, the calculated sequences λ_i and $\bar{m}\, i_i$ for packets extracted from the SMI3 data set are plotted as function of time (the time reference for a packet is its median time), for $M = 30$. Visually, some positive correlation can be noticed, and the estimate of ρ is positive (Table 2); still, it is insignificantly different from zero. The alternative technique of dense/sparse population comparison (Fig. 6a, Table 3) demonstrates its efficiency, indicating the presence of negative correlation between b-value and event density at the significance level of $Q = 6\%$.

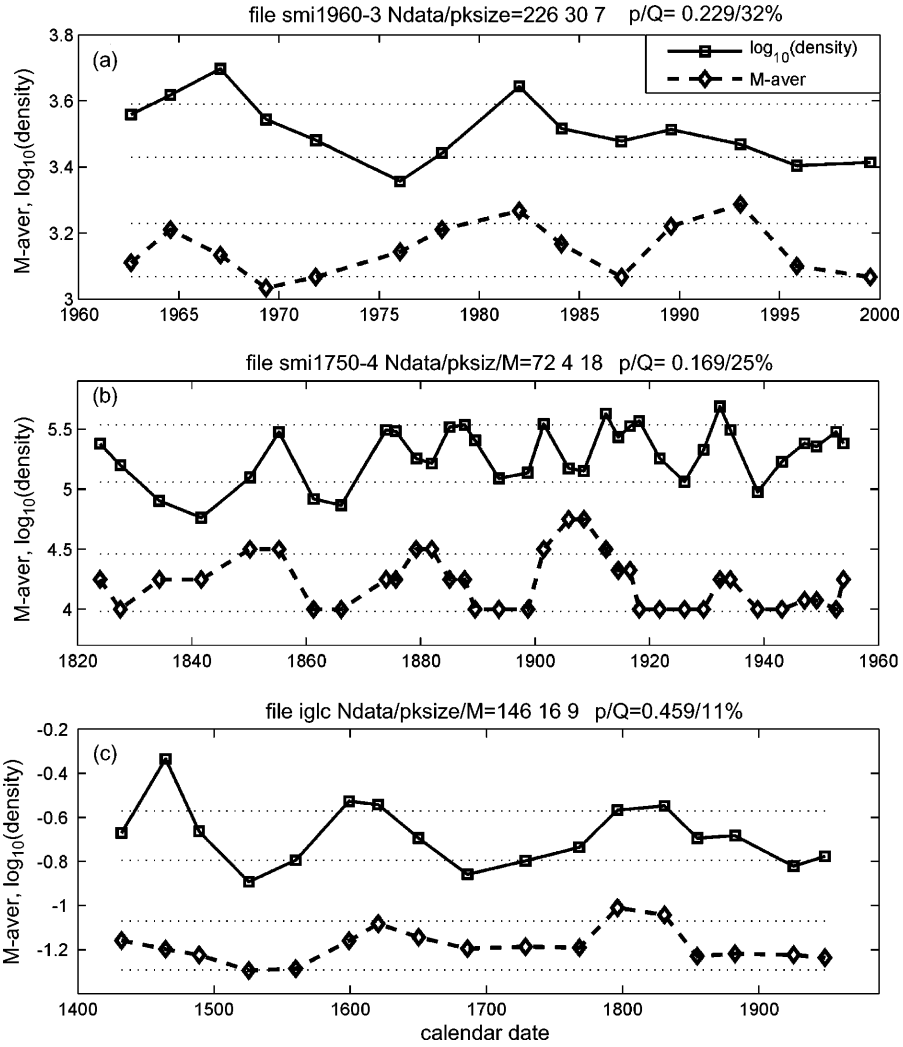

Fig. 5. Comparison of temporal trends of log event rate (solid lines and squares) and of "average magnitude" $\bar{m}$ (dashes and diamonds), for data sets SMI3 (a), SMI4 (b) and IVI(c), estimated using event packets of constant number. See Table 2 for details. Plots for $\bar{m}$ are shifted vertically for visual clarity. Horizontal dot lines indicate approximate $\pm 1\sigma$ corridors assuming no temporal variations.

Table 2
Parameters of correlation between time series of event rate and "average magnitude" $\bar{m}$

Data set, its volume	Packet size M	ρ	Q (%)
SMI3, $N=226$	30	0.22	–
SMI4, $N=72$	4	0.17	–
IVI, $N=146$	6	0.53	0.3
	8	0.46	2.6
	10	0.33	13
	12	0.45	7.2
	14	0.26	23
	16	0.46	11

Table 3
Comparison of b-values between event subsets that occupy time intervals with low and high event rate

Data set	$n_{0.5}$	dt_l (year)	b_l	dt_h (year)	b_h	$\sigma(b)$	Q (%)
SMI3	113	0.27	0.73	0.11	0.63	0.064	5.8
SMI4	36	2.8	0.66	1.01	0.55	0.10	13
IVI	73	6.08	1.84	1.89	1.18	0.18	0.04

$n_{0.5}$, volume of each of the two data subsets; dt_l and b_l, average inter-event interval and b-value estimate for low-rate intervals; dt_h and b_h, same, for high-rate intervals; $\sigma(b)$, rms deviation of b-value estimate; Q, significance level for the hypothesis $b_l > b_h$, obtained by Monte-Carlo simulation.

7.3. SMI 4 data set

The results of correlation analysis are shown in Fig. 5b, and Table 2. Although a marginal significance level was indeed attained for the presented case with $M=4$, this result is unstable at other M and must be considered unreliable. The test with dense/sparse population comparison (Fig. 6b) has no adjustable parameters, so the similar value of significance level obtained in this case can be considered meaningful, and the presence of correlation can be considered as being marginally supported by the SMI4 data set.

7.4. IVI data set

The results are shown on Fig. 5c, for $M=16$. In this case, the pair of estimates ($\rho=0.57$, $Q=5\%$) was obtained. In Table 2, results are listed for this several other values of M. One can see that the inequality $\rho<0$ takes place in a wide range of M values, making the reality of this hypothesis rather probable. Still, the values of Q vary markedly. However, by comparing b-values for dense and sparse populations (Fig. 6c), this result is confirmed rather reliably, at as low a Q value as 0.03% (Table 3).

8. Comparative review of results obtained by various methods

Let us now consider the results of various ways of data analysis. Let us begin with three modes of spectral analysis applied to three data sets, as seen in Fig. 4 and Table 1, viewed as a whole. One evident observation is that the results for the SMI4 data set are, generally, the least convincing. This could be expected: this data set is the smallest in volume, and, containing older data, more prone to problems of calibration and completeness. Thus, one can give less weight to results obtained from this source. Now let us pass to more interesting generalizations.

The first point to note is the difference in the degree of expression of common and order clustering. The expression of common clustering is the weakest: it is observed (at significance levels 14% and 7%) only in two cases out of three, and the α value (here denoted α_{CCl} for this case) averaged over three cases, equals 0.09. (Averaging of α values is performed with weights based on standard deviations $\sigma(\alpha)$ of Table 1; an additional weight factor 0.25 was used with SMI4 data obtained over a narrow frequency band.) Order clustering is the most prominent: it is clearly expressed in each of three cases (at significance levels 2.1%, 11% and 9%), and the α value (denoted α_{OCl}) averaged over three cases, equals 0.20. As for episodicity of VDR, this feature is expressed approximately as well as order clustering, at significance levels of 6%, 16% and 1.7% and with average $\alpha_{VDR}=0.11$.

Generally speaking, each of the two kinds of clustering may alone cause significant episodicity of the VDR. Their correlated action, suggested by the analysis of b-value, can be expected to

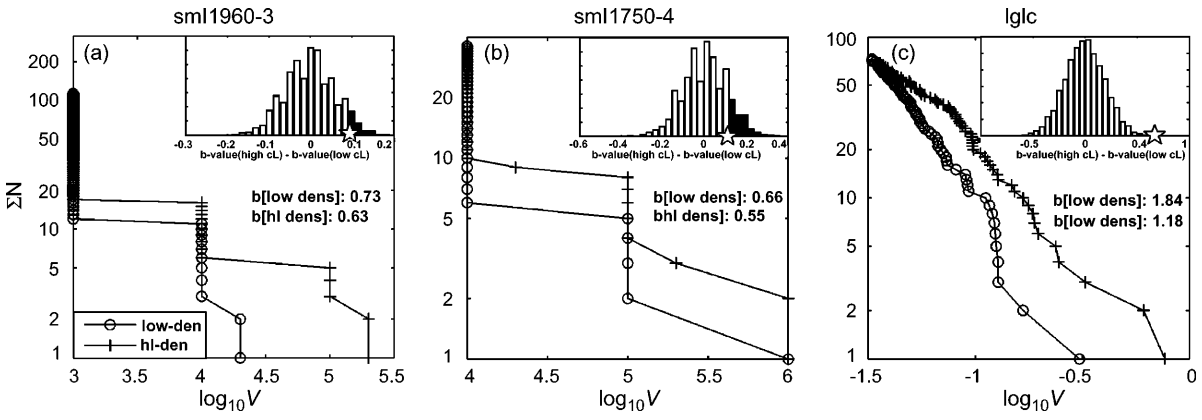

Fig. 6. Cumulative plots of size–frequency distribution for data sets SMI3 (a) SMI4 (b) and IVI (c), separately for events on time intervals with lower and higher event density (see Fig. 2 for analogous plot for non-split data). In inserts: histograms (simulated probability density functions) of the difference of b-value between lower and higher event density intervals, obtained in 10,000 runs of random/surrogate data sequences with no λ–b correlation. Star marks the position of the difference estimates from real data. Sum over black bins makes the significance level; see Table 3.

result in α_{VDR} being larger that any of α_{CCl} or α_{OCl}. This inequality is observed indeed for the IVI data set, but is not the case for both the SMI3 and SMI4 data sets. This is probably the result of statistical fluctuations in our small data sets; with sufficient data, one can seemingly expect that generally, $\alpha_{CCl} < \alpha_{OCl} < \alpha_{VDR}$.

The tendency of negative correlation between *b*-value and event rate, when analyzed in terms of correlation coefficient between "average magnitude" and event rate time series, presents difficulties of detection: it is seen clearly in only one of the three cases studied (Table 2, Fig. 5). The specially designed statistical technique of comparing *b*-values of dense and the sparse populations (Table 3) performs much better, showing the presence of correlation at significance levels of 6%, 14% and 0.03%. These consistent results obtained from independent data sets seem to support the idea of correlation between time histories of common and order clustering. This correlation strongly suggests that common and order clusters are controlled by one and the same factor, causing them to be positively correlated.

9. Discussion

9.1. Fractal episodicity versus alternative models

The results listed above suggest that random fractal clustering is present for global volcanic sequences, most clearly as order clustering and bursty VDR, and less prominently as clustering of event rate. Event rate is the most advanced field of study, with many alternative models proposed; see discussion in the Introduction. One can treat the observed variations of event rate as a manifestation of a point process with time-dependent event rate (deterministic or random). For the cases when random correlated temporal structure is assumed, also various assumptions can be made. Above, the variogram of the analyzed process was implicitly assumed to be the power law one; other variogram models are also possible. Alternatively, one might show that time delays between events are power law or Weibull law distributed. On the whole, there are many modes to analyze the same data, and their non-trivial temporal structure can be expressed in a number of ways. How unique is the way of data description proposed here, and why is the actually employed approach preferable?

The discrimination between various alternative models can be very difficult, and essentially hopeless in the cases under study, with data sets of the size 100–300 events. Thus, there is no hope to obtain a unique model; and to select a particular model for the data sets studied here is, to a substantial degree, a matter of conceptual preference. To justify the actual choice of the model it can be noted that it is based on the very general fractal concept, and has only one adjustable parameter (namely, α). And in terms of this single parameter (with different values) one can describe not only the event rate model ("1(t)") but also two more models—for the volume list ("$V(i)$"), and for VDR function ("$V(t)$"). It must be understood that nothing like a proof is possible to substantiate our particular choice. However, successful data description by means of the selected model gives it a certain support.

9.2. Lack of general understanding of fractal/flicker noise phenomena

Before discussing the possible volcanological meaning of results, some general preliminary notes should be given. Despite the fact that fractal objects, and particularly fractal temporal behavior, was a field of very intensive study in the last 20 years, practically all this study was aimed at *description* of observations; only limited and not very fruitful efforts were directed to *explanations* of such behavior. The same comment is true with respect to the field of flicker noise. Among attempts to explain these phenomena, the one seemingly most publicized is the concept of self-organized criticality (SOC) and its incarnation in the popular "sand-pile model" (Bak et al., 1987; Bak, 1997). Unfortunately, the initial hope that a mathematical sand pile generates avalanches that represent a pulsed flicker noise happened to be premature: spectral representation of the output of a "simple" sand-pile is white noise (Milotti, 2002). Of course, in the general field of SOC and fractals, there are models that do generate flicker noise, but these models typically either include special assumptions that insert some memory in the system, or they find flicker noise in the evolution of intrinsic parameters and not in the output of the system. The origin of flicker noise in the output of a natural system continues to be a first-class enigma in modern physics. And it would be unusually lucky to find a good explanation of presumed fractal clustering/flicker noise behavior in the specific field of volcanic phenomena.

9.3. "Global magma plumbing system": its existence and hierarchy

Sigurdsson (2000) notes that episodicity of VDR (over geological time scale) is a significant fact but do not propose any explanation. As seen from the previous paragraph, experience from other fields of science is also not encouraging. Nevertheless, some speculations seem to be warranted. The revealed facts can be discussed in terms of properties of a hypothetical "global magma plumbing system" (GMPS), considering it as a certain material supply system. It has an output, in the form of eruptions, and it has much less transparent input, that must include subduction-related fluid injection, and/or the inflow of silicate liquid from deep interior, etc. The assumption suggested by the presented results is that despite the fact that the GMPS consists of many spatially distant and seemingly completely hydraulically isolated subsystems, it is capable of synchronizing the operation of these subsystems. If this is so, there are two very general possibilities: either the synchronism is a manifestation of a common "central" controlling factor or a single unifying mechanism; or it is a distributed feature that is related to a certain positive interaction between volcanic regions/subsystems. Any of these two variants may result in seemingly "cooperative" ("epidemic") mode of behavior.

Within the fractal conceptual framework, one can expect to meet a down-scaled version of this global system at the regional scale, to be manifested in a region-wide "cooperative" behavior of volcanic activity of individual volcanic centers. Recently, the Kamchatka region was shown to be a particularly good example

of such an influence (Gusev et al., 2003). All three modes of behavior discussed here for global data, namely, common and order clustering and episodicity of VDR have been found for the catalog of explosive eruptions on Kamchatka over a 10,000 years time span. Moreover, for these data, order clustering was again much more clearly expressed than common clustering. Pelletier (1999) proposed some mechanisms, acting at "roots of volcanoes", that might result in space–time clustering of volcanism at a local to regional scale. However, these models are hardly applicable for the case of global activity.

An alternative statistical model can be imagined that ascribes clustering property of global event sequences to summation of independent but *intrinsically clustered* sequences from individual volcanoes. This explanation is formally correct, e.g., for event sequence represented as non-homogeneous Poisson process with random event rate $\Lambda(t)$. Indeed, assume $\Lambda(t)$ to be a sum of many independent components $\lambda_i(t)$, each of them being an independent flicker noise of a certain exponent α. Each such noise can be considered as white noise passed through the filter $f^{-\alpha/2}$. Consider a long time segment $T \gg \max(1/\lambda_i(t))$. Let us Fourier-transform $\Lambda(t)$ and $\lambda_i(t)$ over T, to result in spectra $\Lambda(f)$ and $\lambda_i(f)$. Then

$$\Lambda(f) = \sum \lambda_i(f) = \sum f^{\alpha/2} w_i(f) = f^{\alpha/2} \sum w_i(f) = f^{\alpha/2} W(f)$$

where $w_i(f)$ and $W(f)$ are Fourier transforms of white noises. We see that $\Lambda(t)$ is a flicker noise again. Models of this kind can be imagined also for order clustering and clustering of VDR, as well as for correlated behavior of order and common clustering.

It must be understood that through the discussed model, an attempt is made to explain by coincidences a very clear phenomenon. For example, during only 5 months in 1991, the two largest, VEI = 5+, eruptions of 1960–2002 took place (Pinatubo and Cerro Leon), separated by a single VEI = 3 event, making the local b-value estimate very low. Attempting to explain this fact by random coincidence of maxima in two unobservable independent $b(t)$ functions for these distant volcanoes does not look reasonable. Similarly, to explain global correlation between common and order clustering one needs to introduce correlated variations of $\lambda_i(t)$ and $b_i(t)$ for each volcano. Although this surprising tendency seems to exist globally, it is highly doubtful for an individual volcano: it means that the larger are eruptions of a volcano, the more frequent they are. On the whole, the concept of summation of many independent flicker noises looks highly artificial. This however is a matter of opinion. A more significant counterargument can be based on the well-established facts that clustering behavior is not merely a temporal phenomenon, it is actually a spatio-temporal one, demonstrated over spatial scales from tens to several thousands of kilometers (Condit and Connor, 1996; Pelletier, 1999). The observed space–time correlation definitely contradicts the idea of independent event fluxes that predicts no correlation between time series for non-intersecting sub-areas. Hence, explanations of obtained results based on random coincidence of intrinsically clustered single-volcano sequences are not considered plausible and are not discussed more.

9.4. "Global magma plumbing system": what we understood about its properties

Now let us consider some primitive variants of possible behavior of the GMPS. Imagine a hypothetic GMPS whose average input rate is a certain continuous, constant or weakly oscillating function of time. As for the output of GMPS, we know that it consists of short pulses or eruption events. Assume also that the total volume of the GMPS is limited. Then, the average throughput of the system (in the assumed stationary mode of operation) must be weakly varying as well. Now assume that, for some reason, the mean output event rate varies in time (thus, the common clustering is assumed). To fulfill the constraint of a constant throughput, during the intervals of maxima of event rate the average event size must be relatively low. Conversely, when events are infrequent, their size must be relatively large. This is schematically shown on Fig. 7 as Case A. In such a case, large events do not occur in random order but (1) inevitably form groups, and (2) these groups coincide with periods of *low* event rate. Therefore, order clusters arise automatically in this case, but they arise *in antiphase* with respect to common clusters.

For the alternative ideal model (Fig. 7, Case B), assume that the input to the GMPS (still with limited volume) is in itself a deeply non-stationary, "bursty", but still continuous time function. The near-surface volcanic conduits must let pass through these bursts, converting them into individual pulses. Generally speaking, these conduits can use the following strategies to pass an arriving burst of material: (1) to increase eruption rate, keeping mean eruption size constant; (2) to increase mean eruption

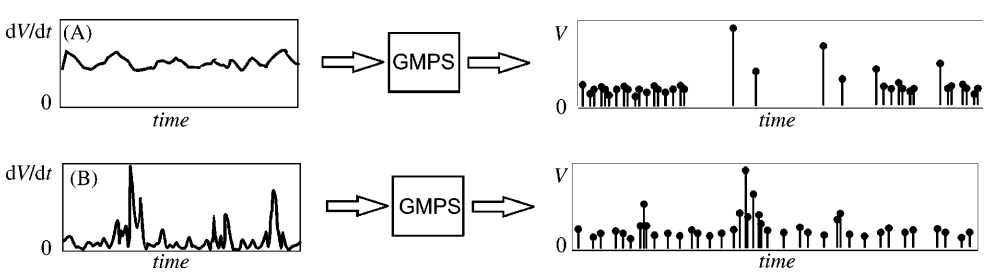

Fig. 7. A sketch showing two hypothetic modes of behavior of the global magma plumbing system. (Top) The case of modestly varying input material rate and the limited volume of the plumbing system proper; the output discharge pulses are frequent when they are small, and rarified when they become larger; negative order clustering results. (Bottom) Wildly varying input material rate and, again, the limited volume of the plumbing system proper. In agreement with observations, discharge pulses are larger when they are more frequent, and positive order clustering arises.

size, keeping eruption rate constant; (3) to combine strategies (1) and (2). Strategy 3 looks the most probable, making common clusters and order clusters likely to arrive *in phase*. And this is just what we observe in volcanic event catalogs: "average magnitude" is positively correlated with event rate. This speculation suggests the real GMPS may be fed in an intermittent manner.

One can also imagine that the GMPS is of effectively infinite volume, and also is capable to convert the approximately stationary (constant rate) input into episodic, intermittent output. Generally, this reasoning is as acceptable as the previous one, However, it does not give us anything essentially new: such a "big" GMPS can be logically separated into the first, voluminous and burst-generating stage, and the second stage of limited volume that is equivalent to the entire GMPS considered in the previous paragraph.

Of course, this speculation does not take us too far; but two interesting deductions still follow. First an important conclusion is that the GMPS seems *to exist*, a conclusion that is very far from being evident.

The second corollary is that the complete system that consists of the GMPS and its inputs as a whole has an inherently intermittent behavior, and its volume is seems to be unlimited. This formal deduction should not be understood literally: an upper limit of volume of the GMPS must exist (see e.g., Mason et al., 2004). When cluster size approaches this upper limit, the clustering behavior must disappear.

9.5. On long-term memory

Often, flicker noise behavior, or pink power spectra, with $\alpha > 0$, are considered as long-range dependent or long memory processes (Beran, 1994), because correlation persists for arbitrary long delays. In other words, clusters of any (including very long) duration are present. (Often, processes with long memory are characterized by the Hurst parameter $H = (1 + \alpha)/2$.) Over the time scales analyzed here, of 1–500 years, the above results indeed can be interpreted in this way: global volcanic processes do have long memory. Combining the results with other published data, this conclusion can be generalized for much longer time scales (e.g., up 10^8 years following Pelletier, 1999).

9.6. Possible applications

The obtained results are highly significant for understanding the impact of volcanism on climate. The simplest approach in analyzing this impact is to assume that individual eruptions of variable size arrive as a Poissonian sequence, or maybe as a clustered sequence with a finite, limited correlation time. Taking into account fractal clustering, with long memory, can significantly modify the estimates. An important point is that the easily perceptible phenomenon of common clustering (clustering of dates) may be of less relevance to climatic change than order clustering (clustering of sizes) that seems to be more prominently expressed.

The phenomenon of fractal clustering is significant also for volcanic hazard assessment. Assume that for a certain volcanic center, fractal clustering behavior can be expected. On a qualitative level, this assumption means that the observed event rate or VDR, even when it is based on apparently sufficient volume of data (statistics of events, etc.), cannot be safely extrapolated to future and used as a reliable estimate for future activity. Changes of the current activity level, both to significantly lower or to significantly higher levels, must always be considered as realistic alternative scenarios. With some efforts, quantitative approaches for such "non-stationary" scenarios can be developed.

10. Conclusions

From three independent approximately homogeneous data sets, three kinds of volcanic eruption time sequences were constructed: (1) of events as unit-mass points on the time axis, (2) of event volume versus sequential number in the time-ordered list, and (3) of variable size events as massive points on the time axis. Sequences of all tree kinds show indications of clustering behavior, denoted in these three cases as (1) common clustering, (2) order clustering and (3) clustering of volcanic discharge rate, or VDR.

For two data sets out of three, the clustering behavior can be considered to be self-similar (fractal). Spectral analysis has shown that sequences from these two data sets can be considered as flicker noises. For the three listed kinds of sequences, the average values of power spectral exponent are equal to -0.09, -0.19 and -0.11, respectively.

The hypothesis of positive correlation in time for common and order clustering was checked by testing negative correlation between time series of event rate and of b-value, or the exponent in the power law for size–frequency distribution of eruptions. Two techniques of statistical analysis of this correlation were applied. The first of them was intuitively more attractive but less efficient as a statistical tool; another showed clear manifestations of the named correlation in all three data sets analyzed.

Comparing the present work with earlier results, one can conclude that order clustering, episodic/intermittent VDR, and, to a less degree, common clustering may be characteristic properties of volcanic process, both on global and regional scales.

The obtained results give a reasonable description of data, but do not give clear clues regarding causes of the revealed peculiarities. One relatively certain conclusion, vague in details but still quite radical, is that to provide the revealed coordinated behavior of volcanic time series over entire Earth, some global mechanism or mechanisms must exist.

Acknowledgements

I am grateful to Vera Ponomareva, David Pyle and Steve McNutt for valuable criticism and many suggestions that significantly improved the manuscript.

References

Aki, K., 1965. Maximum likelihood estimates of b in the formula $\log N = a - bM$ and its confidence limits. Bull. Earthquake Res. Inst. Univ. Tokyo 43, 237–239.

Ammann, C.M., Naveau, P., 2003. Statistical analysis of tropical explosive volcanism occurrences over the last 6 centuries. Geophys. Res. Lett. 30, 1210, doi:10.1029/2002GL016388.

Bak, P., 1997. How Nature Works. The Science of Self-organized Criticality. Copernicus, New York.

Bak, P., Tang, C., Weisenfeld, K., 1987. Self-organized criticality: an explanation of $1/f\psi$ noise. Phys. Rev. A 38, 364–374.

Bebbington, M.S., Lai, C.D., 1996. On nonhomogeneous models for volcanic eruptions. J. Math. Geol. 28, 585–600., doi:10.1007/BF02066102.

Beran, J., 1994. Statistics For Long-Memory Processes. Chapman and Hall, 331 pp.

Cambray, H., Cadet, J.-P., 1996. Synchronisme de l'activite volcanique d'arc: mythe ou realite? C. R. Acad. Sci. Paris 322, 237–244, ser IIa.

Condit, C.D., Connor, B.C., 1996. Recurrence rates of volcanism in basaltic volcanic fields: an example from the Springerville volcanic field, Arizona. Geol. Soc. Am. Bull. 108, 1225–1241.

Connor, B.C., Hill, B.E., 1995. Three non-homogeneous Poisson models for the probability of basaltic volcanism: application to the Yucca Mountain region, Nevada. J. Geophys. Res. 100 (B6), 10,107–10,125.

Dubois, J., Cheminee, J.-L., 1988. Fractal analysis applied to the sequence of volcanic eruptions of Piton de la Fournaise (La Reunion Island): Cantor dust model. C. R. Acad. Sci. Paris 307, 1723–1729.

Dubois, J., Cheminee, J.-L., 1991. Fractal analysis of eriptive activity of some basaltic volcanoes. J. Volcanol. Geotherm. Res. 45, 197–208.

Dubois, J., Cheminee, J.-L., 1993. Piton de la Fournaise volcano eruptive cycles: fractal analysis, attractors, deterministic aspects. Bull. Soc. Geol. France 164, 3–16.

Godano, C., Civetta, L., 1996. Multifractal analysis of Vesuvius volcano eruptions. Geophys. Res. Lett. 23, 1167–1170.

Gusev, A.A., 2005. Multiscale order grouping in sequences of Earth's earthquakes. Izvestiya, Phys. Solid Earth. 41, 798–812 (original in Russian: Fizika Zemli, 2005, No. 10, 30–45).

Gusev, A.A., Ponomareva, V.V., Braitseva, O.A., Melekestsev, I.V., Sulerzhitsky, L.D., 2003. Great explosive eruptions on Kamchatka during the last 10 000 years: self-similar irregularity of the output of volcanic products. J. Geophys. Res. 108 (B2), 2126, doi:10.1029/2001JB000312.

Guttorp, P., Thompson, M.L., 1991. Estimating second-order parameters of volcanicity from historical data. J. Am. Stat. Assoc. 86, 578–583, doi:10.2307/2290385.

Ho, C.-H., 1991. Non-homogeneous Poisson model for volcanic eruptions. Math. Geol. 23, 91–98.

Ho, C.-H., Smith, E.I., Feuerbach, D.L., Naumann, T.R., 1991. Eruptive probability calculation for the Yucca Mountain site, USA: statistical estimation of recurrence rates. Bull. Volcanol. 54, 50–56.

Jaquet, O., Carniel, R., 2001. Stochastic modelling at Stromboli: a volcano with remarkable memory. J. Volcanol. Geotherm. Res. 105, 249–262.

Jones, G., Chester, D.K., Shooshtarian, F., 1999. Statistical analyses of the frequency of eruptions at Furnas Volcano, Sao Miguel, Azores. J. Volcanol. Geotherm. Res. 92, 31–38.

Kennett, J.P., McBirney, A.R., Thunell, R.C., 1977. Episodes of Cenozoic volcanism in the circum-Pacific region. J. Volcanol. Geotherm. Res. 2, 145–163.

Makarenko, G.F., 1982. Bursts of trap volcanism in Mesozoic and Cenozoic. Vulcanol. Seismol. (4), 65–77.

Mandelbrot, B.B., 1982. The Fractal Geometry of Nature. W.H. Freeman, New York, 468 pp.

Mandelbrot, B.B., 1999. Multifractals and $1/f$ Noise: Wild Self-Affinity in Physics (1963–1976). Springer.

Mason, B.G., Pyle, D., Dade, B., Jupp, T., 2004. Seasonality of volcanic eruptions. J. Geophys. Res. 109 (B4), B04206.

Milotti, E., 2002. $1/f$ noise: a pedagogical review. URL: http://arxiv.org/abs/physics/0204033.

Ogata, Y., Abe, K., 1991. Some statistical features of the long-term variation of the global and regional seismic activity. Int. Stat. Rev. 59 (2), 139–161.

Pelletier, J.D., 1999. Statistical self-similarity of magmatism and volcanism. J. Geophys. Res. 104 (B7), 15,425–15,438.

Pisarenko, V.F., Pisarenko, D.V., 1991. Spectral properties of multifractal measures. Phys. Lett. A 153 (4–5), 169–172.

Prueher, L.M., Rea, D.K., 2001. Tephrochronology of the Kamchatka-Kurile and Aleutian arcs: evidence for volcanic episidicity. J. Volcan. Geotherm. Res. 106, 67–87.

Rea, D.K., Scheidegger, K.F., 1979. Eastern Pacific spreading rate fluctuation and its relation to Pacific area volcanic episodes. J. Volcanol. Geotherm. Res. 5, 135–148.

Robock, A., 2000. Volcanic eruptions and climate. Rev. Geophys. 38, 191–219.

Robock, A., Free, M.P., 1996. The volcanic record in ice cores for the past 2000 years. In: Jones, P.D., Bradley, R.S., Jouzel, J. (Eds.), Climatic Variations and Forcing Mechanisms of the Last 2000 Years. Springer-Verlag, New York, pp. 533–546.

Siebert, L., Simkin, T., 2002. Volcanoes of the World. . . http://www.volcano.si.edu/gvp/world/.

Sigurdsson, H. (Ed.), 2000. Encyclopedia of Volcanoes. Academic Press, San Diego, California, 1417 pp.

Simkin, T., 1993. Terrestrial volcanism in space and time. Ann. Rev. Earth Planet. Sci 21, 427–452.

Simkin, T., Siebert, L., 1994. Volcanoes of the World, 2nd ed. Geoscience Press, Tucson, Arizona.

Telesca, L., Cuomoa, V., Lapenna, V., Macchiato, M., 2002. Time-clustering analysis of volcanic occurrence sequences. Phys. Earth Planet. Interiors 131, 47–62.

Turcotte, D.L., 1992. Fractals and Chaos in Geology and Geophysics. Cambridge Univ. Press, New York, 78 pp.

Wickman, F.E., 1966. Repose patterns of volcanoes. I. Volcanic eruptions regarded as random phenomena. Ark. Miner. Geol. 4, 291–301.